

SEDIMENT TRANSPORT MODELLING FOR COASTAL MORPHODYNAMICS

A.G. Davies¹ and C. Villaret²

Abstract: The accurate prediction of sand transport rates in the coastal zone depends not only upon the choice of sediment transport model but also, rather critically, upon the formulation used to predict the bed roughness (k_s). Sand transport rates are modelled here using both a One-equation, turbulence-closure, TKE-model and also Bijker's sand transport model. Following some remarks about the nature and importance of sand ripples, results corresponding to wide ranges of wave and current conditions are obtained based upon both prescribed and predicted values for k_s . The substantial difference between the respective results highlights the importance of predicting k_s as accurately as possible in situations in which the bed roughness is not known. An example involving waves incident on a plane sloping beach is used to illustrate the variations in ripple dimensions, and hence k_s , likely to be found in a typical coastal domain. Here Bijker's model has been implemented within the TELEMAC Modelling System to predict the longshore sand transport rate. The inclusion of *local* variations in k_s within the study area approximately halves the longshore transport rate compared with results based on the use of a constant, prescribed value of k_s throughout the domain. The possible consequences of bed roughness variations are discussed briefly in the context of morphological modelling.

INTRODUCTION

The accurate quantification of local sand transport rates in the marine coastal environment is a prerequisite for the prediction of seabed changes and coastline evolution. In an intercomparison with laboratory data in the EU MASTII G8-M Project (1992-5), it was found that four different 'research' models predicted net sediment transport rates beneath asymmetrical waves, and also in collinearly combined wave and current flows, to well within a factor of 2 of the measured values (Davies et al., 1997). In addition, cycle-mean sediment concentration profiles were predicted to good accuracy. However, the range of conditions investigated was quite narrow, involving sheet flow (i.e. plane beds) only. A more recent series of model intercomparisons, and model comparisons with field data, carried out over a wider range of conditions during the EU MASTIII SEDMOC Project (1998-2001), suggested far less convincing agreement between the models and the data, and indicated that large gaps still remain in our knowledge of sand transport processes (Davies et al., 2002).

Initially, in the SEDMOC study, seven 'research' models were intercompared over a wide range of wave and current conditions, corresponding to both plane and rippled sand beds. These models included both one-dimensional vertical (1DV) formulations, varying in complexity from eddy viscosity and mixing length models to a full two-phase flow formulation, and also 2DHV formulations capable of representing vortex shedding above sand

-
- 1) School of Ocean Sciences, University of Wales (Bangor), Menai Bridge, Anglesey LL59 5AB, UK. a.g.davies@bangor.ac.uk
 - 2) Laboratoire National d'Hydraulique et Environnement, Electricité de France, 6 quai watier, BP 49, 78400 Chatou, France. catherine.villaret@edf.fr

ripples. The model results showed greatest convergence for cases involving plane beds, with predicted sand transport rates agreeing to well within an order of magnitude, and greatest divergence for cases involving rippled beds. A similar intercomparison involving (mainly) ‘practical’ sand transport models, carried out over wide wave and current parameter ranges, also showed greatest variability in cases involving rippled beds. Finally, (mainly) practical models were compared with field data obtained at five contrasting field sites. The results showed that suspended sand concentrations in the bottom metre of the flow were predicted within a factor of 2 of the measured values in 13% to 48% of the cases considered, and within a factor of 10 in 70% to 83% of the cases, depending upon the model used. Estimates of the measured longshore component of suspended sand transport yielded agreement to within a factor of 2 in 22% to 66% of cases, and within a factor of 10 in 77% to 100% of cases, again depending upon the model used.

The results of the SEDMOC study suggested that, at the present stage of research, considerable uncertainty should be expected if untuned models are used to make *absolute* predictions for field conditions, and that the availability of some measurements on site is still a necessary requirement for high-accuracy sand transport predictions. However, for morphological modellers, the results were considered to be more encouraging, since many of the models exhibited agreement in their *relative* behaviour over wide ranges of wave and current conditions, which is a prerequisite to obtaining correct morphodynamic predictions.

In the present paper, the importance of the bed roughness (k_s) is highlighted in relation to sediment transport computations. Following a discussion of the general role of sand ripples, a procedure is outlined for the prediction of the dimensions of ripples and, hence, of the bed roughness, in combined wave-current flow. Results are then presented that illustrate the sensitivity of the sediment transport rate to the choice of k_s over a range of wave-current conditions. Finally, an illustrative example is presented involving waves that are incident, both normally and obliquely, on a beach. The variability in the predicted bed roughness k_s as the waves shoal and then break is illustrated. In the case of oblique wave incidence, the effect on the longshore sand transport rate of the use of a locally predicted bed roughness, as opposed to a constant (specified) bed roughness over the entire domain, is demonstrated. The wider implications of these results for morphological modelling are discussed briefly.

SAND RIPPLES AND BED ROUGHNESS

One of the central considerations involved in obtaining reliable sediment transport rate predictions is the accurate specification of the bed roughness. In practice, depending upon the local wave-current conditions and seabed composition, potentially significant variations in the roughness may occur within a coastal area. For example, in deeper water where the wave conditions are relatively inactive, steep sand ripples may occur while, in shallower water where the waves become nonlinear and ultimately break, low ripples or plane bed conditions are likely to be found. If a morphological model does not account for the consequent local variations in bed roughness, significant errors may arise in the pattern of transport rates throughout the study area.

Since large areas of the seabed comprise relatively steep sand ripples, it is unfortunate that, as noted above, our present ability to model the transport above rippled beds is less certain than above plane beds. This is true of both practical formulations, and also detailed research models. In practice, some of this uncertainty arises from the choice of the bed roughness. However, at least in the case of research models, further uncertainty can arise from the way in which reference concentration formulae (or pick up functions) are implemented by modellers above rippled beds. In the SEDMOC study, this latter uncertainty led to variations in the predicted transport rate of between 1 and 2 orders of magnitude (Davies et al., 2002).

There is an essential difference between the sediment transport processes that occur above rippled and plane sand beds (see, for example, Nielsen, 1992; Fredsøe and Deigaard, 1992; Van Rijn et al., 2001). It is important therefore to define the boundary delineating these regimes. Steep ripples are formed by relatively low waves in relatively deep water (i.e. typical offshore conditions). Such ripples tend to be long crested (two-dimensional), and have steepness (η/λ) greater than about 0.15, where η and λ are the ripple height and length, respectively. The ‘roughness’ (k_s) of a rippled bed is normally equivalent to about 3-4 ripple heights ($k_s = 3\eta - 4\eta$). Beneath steeper waves in shoaling water, the ripples start to become shorter crested (transitional 2D-3D profiles); here their steepness decreases, causing k_s to decrease. Finally, beneath very steep and breaking waves, the ripples may be ‘washed out’ completely, the bed becomes plane (‘sheet flow’ regime), and k_s decreases still further (scaling on the sand grain diameter). This sequence is summarised in Table 1 below in terms of the non-dimensional ‘relative roughness’ A_0/k_s , where A_0 is the near-bed orbital excursion amplitude. For cases of practical interest in the sea it is possible to associate with the respective ranges of A_0/k_s , equivalent approximate ranges of wave Reynolds number RE ($=A_0^2\omega/\nu$), where ω = wave angular frequency and ν = kinematic viscosity, as indicated in Table 1. The type of oscillatory boundary layer flow expected in different ranges of A_0/k_s and RE has been reviewed by Davies and Villaret (1997).

Table 1. Bed form characteristics in the coastal zone

Bed form characteristics	2D Steep Ripples	2D and 3D Low Ripples	Washed-out Ripples	Plane Bed
Ripple steepness η/λ	$\eta/\lambda \geq 0.15$	$0.05 < \eta/\lambda \leq 0.15$	$\eta/\lambda < 0.05$	$\eta/\lambda = 0$
Relative roughness A_0/k_s	O(1)	O(1-10)	O(10-100)	O(100-1000)
Reynolds number RE	O(10^3 - 10^4)	O(10^4 - 10^5)	O(10^5)	O(10^6 - 10^7)

Above plane beds in oscillatory flow, momentum transfer occurs primarily by turbulent diffusion and may, together with the associated sediment transport, be modelled using, for example, conventional turbulence-closure, numerical, schemes. In contrast, above rippled beds, momentum transfer and the associated sediment dynamics are dominated in the near-bed layer by coherent motions, specifically by the process of vortex formation above ripple lee slopes, and the shedding of these vortices at flow reversal. Above steep, long-crested ripples, with $\eta/\lambda \geq 0.12$, this well-organised, ‘convective’ process of vortex formation and shedding is highly effective in entraining sand into suspension. The rough turbulent oscillatory boundary layer above rippled beds is considerably thicker than that above plane beds, the boundary layer consisting of a lower layer dominated by the vortex shedding process and an upper layer in which the coherent motions break down into random turbulence. This leads to the entrainment

of sediment into suspension to considerably greater heights than above plane beds. In combined wave and current flow above ripples, the outer part of the boundary layer structure merges with the turbulent ‘current’ boundary layer, into which sediment can be entrained into suspension to still greater heights.

Several modelling studies of two-dimensional horizontal-vertical (2DHSV) oscillatory flow above rippled beds have sought to represent the formation and shedding of vortices, and the subsequent trajectories of the (decaying) vortices (Longuet-Higgins, 1981; Blondeaux and Vittori, 1991; Hansen et al., 1994; Malarkey and Davies, 2002). Sediment in suspension above ripples has been modelled by Hansen et al. (1994), Block et al. (1994), and Andersen and Fredsøe (1999). Although such 2DHSV-models have achieved reasonable success in representing the main features of vortex dynamics and the associated sediment transport above rippled beds, they are unduly complex from an engineering point of view. For the most part, existing engineering models attempt to represent ripples by simply enhancing the bed roughness k_s used in standard, one-dimensional vertical (1DV) ‘flat bed’ formulations. This approach has some merit for low ripples (Davies and Villaret, 2000), but has severe conceptual limitations for steep ripples. Appropriate time-mean formulations for the eddy viscosity and sediment diffusivity above rippled beds, for use in a horizontally-averaged 1DV framework, have been proposed by Nielsen (1992) and Sleath (1991), and by Nielsen (1992), respectively. They presented empirical evidence to show that, in contrast to the plane bed case, a height-independent mean viscosity is appropriate in the near-bed vortex layer above ripples. Subsequently, it was shown by Davies and Villaret (1997, 1999) that time-variation in the eddy viscosity is more pronounced above ripples than above plane beds, with peaks in viscosity occurring near times of flow reversal. Davies and Thorne (2002) have presented recently a relatively simple, 1DV modelling approach that includes a time-varying eddy viscosity of this type. This model represents both intra-wave flow and sediment transport processes, and also the near-bed wave-generated residual currents above the ripples.

ESTIMATION OF BED ROUGHNESS (k_s)

Davies and Villaret (2000) suggested the following procedure for the calculation of the bed roughness k_s in combined wave-current flow, based on the formulations of Wiberg and Harris (1994) and Tanaka and Dang (1996). Since the strength of any mean current present at the edge of the (thin) oscillatory boundary layer is relatively small (Fredsøe et al., 1999), the waves may be taken as the starting point in the estimation of the bed roughness. The formulation of Wiberg and Harris (1994) for waves alone has thus been used initially to calculate the wavelength (λ) and steepness (η/λ) of the seabed ripples. A non-iterative procedure for the calculation of η and λ using Wiberg and Harris’ formulation has been presented recently by Malarkey and Davies (2003).

To allow for the superimposition of a current on the waves, the orbital diameter d_0 ($=2A_0$) is next replaced by αd_0 using the parameter α proposed by Tanaka and Dang (1996) for collinear wave-current flows. This has been extended to allow for the superimposition of waves on a current at any angle of attack. Moreover, in order to ensure that the ripples in general angular cases are not unrealistically steep when, for example, a strong current is combined perpendicularly with low waves, a ‘maximum steepness’ criterion $(\eta/\lambda)_{\max} = f(\theta'_{\max})$

has been imposed (θ'_{\max} = peak, skin friction, Shields parameter). The function $f(\theta'_{\max})$ used is similar to Nielsen's (1992) expression. Finally, the predicted values of η and λ have been used to define the bed roughness (k_s). In the TKE-model, discussed shortly, the following rule has been adopted:

$$k_s = 25\eta(\eta/\lambda) + 50'D$$

where the terms on the right hand side represent respectively the ripple roughness and the mobile bed roughness (D = grain diameter). In Bijker's (1971) model, also discussed below, the specified rule $k_s = \max(\eta, D_{90})$ has been used.

USE OF PRESCRIBED VERSUS PREDICTED k_s IN THE CALCULATION OF SAND TRANSPORT RATES

To illustrate the sensitivity of sediment transport rate predictions to the choice of bed roughness k_s , results are presented here based upon both prescribed and predicted values of k_s . Two models are considered: i) the 'TKE-model' of Davies and Li (1997) and ii) Bijker's (1971, see also 1992) sand transport model.

The 'TKE model' is a local, one-dimensional (vertical) numerical formulation, based on a One-Equation, turbulent kinetic energy (TKE) closure. The model, which predicts both intra-wave and cycle-mean sediment concentrations and fluxes, has been (i) adapted to allow it to be run in 'flat bed' cases ($\eta/\lambda \leq 0.12$) with any prescribed or predicted bed roughness k_s , and (ii) extended to allow it to be run in 'rippled bed' cases ($\eta/\lambda \geq 0.12$). Further details about the implementation of this model have been given by Davies and Villaret (2000, 2002).

Bijker's (1971) model is used widely by practising engineers due to its ready implementation and also the fact that its predictions are broadly similar to those of more complicated, practical models. It also has the appeal of being based on classical concepts for the bed load and suspended load, rather than relying on empirical curve fitting to transport data. [In the present implementations, Bijker's coefficient b has been taken as $b = 5$.] Bijker's model takes account of the presence of ripples on the bed simply through the prescription of k_s . However, the determination of ripple height (η) is left to the user. As noted by Davies and Villaret (2000), for combined waves and currents the formulation adopted by Bijker for the mean shear stress is highly non-linear, particularly for waves superimposed on weak currents.

The comparisons in this section involve several currents alone, and four waves combined with these currents at an angle of attack of $\pi/2$ in water of depth 5 m, temperature 15° and salinity 0‰. The parameter settings are those used originally by Van Rijn (1993, Appendix A). As shown in Table 2, the depth-mean velocity (U_c) varies in the range 0.1-2 ms^{-1} . The four waves, referred to as 'Waves 1 to 4', are defined by their significant heights (H_s) and peak periods (T_p). Following the approach of Van Rijn (1993) the waves have been treated as purely sinusoidal, and near-bed wave velocity amplitudes (U_w) have been calculated using linear wave theory as 0.255, 0.568, 1.207 and 1.879 ms^{-1} , respectively. The seabed sediment comprises sand having $D_{50} = 0.25$ mm and $D_{90} = 0.5$ mm. The bed roughness has been *prescribed* by Van Rijn (1993) as representative of field conditions, all of the prescribed values of k_s in Table 2 being considerably larger than the granular roughness $k_s = 2.5D_{50} = 0.625$ mm. For the current alone, and the current combined with the two smaller waves, the

roughness varies from $k_s = 0.1$ m ('rippled bed') to 0.02 m ('flat bed'). For the current combined with the two larger waves, the (minimum) flat bed roughness of 0.02 m is imposed throughout. In the flat bed cases, the sand size in suspension (D_s) is taken as the median size of the bed material ($D_s = D_{50}$); for the rougher beds in less active wave-current conditions, D_s ($< D_{50}$) is as specified in Table 2. The settling velocity (w_s) corresponding to D_s has been calculated using the formula of Van Rijn (1993).

Table 2. Parameter settings (c.f. Van Rijn, 1993) for runs with prescribed k_s and D_s

Current Alone					
$H_s = 0$ m					
Waves 1&2			Waves 3&4		
$H_s = 0.5$ m			$H_s = 2.0$ m		
$T_p = 5$ s			$T_p = 7$ s		
$H_s = 1.0$ m			$H_s = 3.0$ m		
$T_p = 6$ s			$T_p = 8$ s		
Depth-mean current vel. U_c (m/s)	Bed roughness k_s (m)	Suspended sand size D_s (mm)	Depth-mean current vel. U_c (m/s)	Bed roughness k_s (m)	Suspended sand size D_s (mm)
0.1	0.1	0.17	0.1	0.02 (flat)	0.25
0.3	0.1	0.17	0.3	0.02 (flat)	0.25
0.5	0.1	0.17	0.5	0.02 (flat)	0.25
0.6	0.1	0.18	0.6	0.02 (flat)	0.25
0.7	0.1	0.19	0.7	0.02 (flat)	0.25
0.8	0.1	0.2	0.8	0.02 (flat)	0.25
1.0	0.1	0.21	1.0	0.02 (flat)	0.25
1.2	0.08	0.22	1.2	0.02 (flat)	0.25
1.5	0.06	0.23	1.5	0.02 (flat)	0.25
1.8	0.03	0.24	1.8	0.02 (flat)	0.25
2.0	0.02 (flat)	0.25	2.0	0.02 (flat)	0.25

In Figure 1, the TKE-model results based on the prescribed k_s values are presented. The five full lines show the total transport rates (Q_t) predicted by the TKE-model for the current alone and, successively, for the current in combination with the four waves. The effect of waves on the transport rate is substantial, particularly for waves combined with the smaller currents. Here the predicted effect of wave stirring is to increase the transport rate by two (or more) orders of magnitude. The equivalent set of dashed curves in this figure represents the transport rates resulting from the use of a granular roughness, given here by $k_s = 2.5D_{50}$. There is up to an order of magnitude difference between the results obtained by assuming a rippled-bed rather than a granular roughness.

In Figure 2 the effect on the transport predictions in Figure 1 of using predicted rather than prescribed values of the bed roughness k_s is illustrated. Here, as part of each calculation, the model has determined the value of k_s . The k_s -values listed in Table 3 correspond to steeply rippled beds for relatively inactive wave and current conditions, through to almost-plane beds for more active conditions, in qualitative agreement with the trends in Table 2. However, due to the variations between the two sets of k_s -values (in Tables 2 and 3), the results for transport rate in Figure 2 exhibit a complex pattern, with rippled beds tending to enhance transport and plane beds tending to inhibit transport, as revealed by the overlapping of the transport curves. This is in contrast to the non-overlapping transport curves in Figure 1 based on the prescribed k_s values. In connection with Figure 2, it should be added that the TKE-model also determined within each run the median diameter (D_s), and hence settling velocity, of the suspended

sediment. The procedure used to obtain the D_s values listed in Table 3 has been explained by Davies and Villaret (2000, 2002).

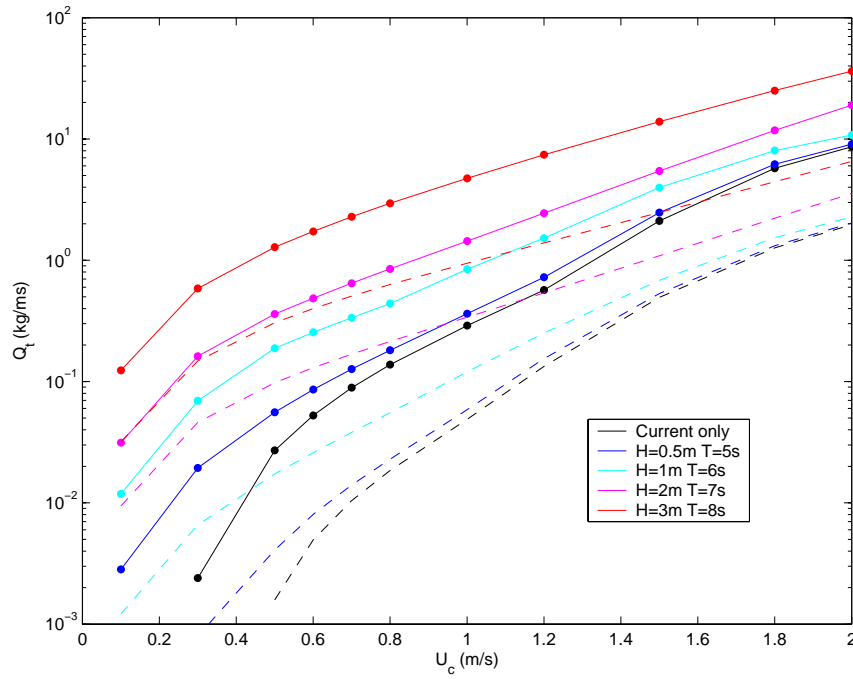


Fig. 1. Total transport rates predicted by the TKE-model with the roughness (k_s) prescribed as in Table 2.

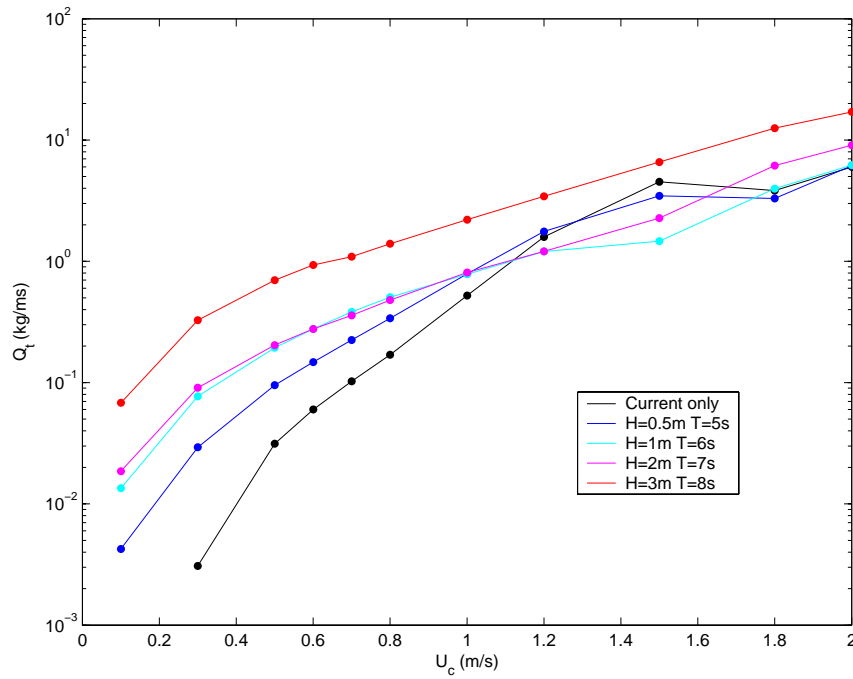


Fig. 2. TKE-model results equivalent to those in Fig.1, but with k_s predicted using the procedure of Davies and Villaret (2000).

Table 3. TKE model input parameters, including predicted k_s and D_s , for the currents combined with Waves 1 & 3

Current + Wave 1 $H_s=0.5$ m $T_p=5$ s			Currents + Wave 3 $H_s=2.0$ m $T_p=7$ s		
Depth-mean current vel. U_c (m/s)	Bed roughness k_s (m)	Suspended sand size D_s (mm)	Depth-mean current vel. U_c (m/s)	Bed roughness k_s (m)	Suspended sand size D_s (mm)
0.1	0.182	0.108	0.1	0.0024	0.224
0.3	0.179	0.113	0.3	0.0024	0.224
0.5	0.163	0.126	0.5	0.0024	0.225
0.6	0.159	0.135	0.6	0.0024	0.225
0.7	0.147	0.143	0.7	0.0024	0.226
0.8	0.132	0.152	0.8	0.0025	0.226
1.0	0.0901	0.169	1.0	0.0026	0.228
1.2	0.0433	0.184	1.2	0.0027	0.230
1.5	0.0059	0.202	1.5	0.0030	0.233
1.8	0.0017	0.216	1.8	0.0033	0.236
2.0	0.0019	0.223	2.0	0.0035	0.238

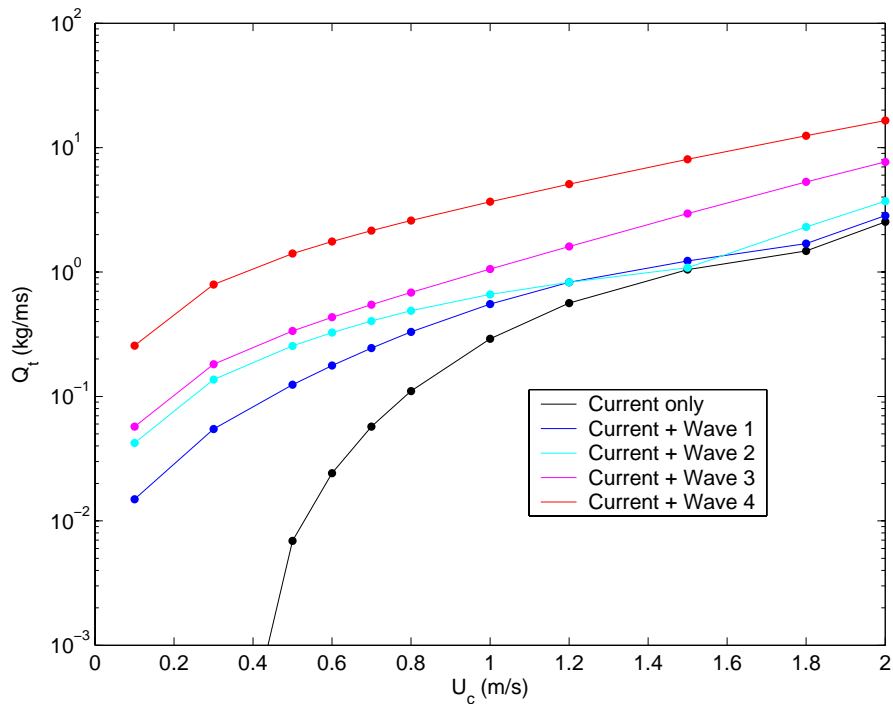


Fig. 3. Results equivalent to those in Fig. 2 based on Bijker's (1991) sand transport model with prescribed values of roughness k_s .

In Figure 3 equivalent transport results are presented based on Bijker's model. Here the same values of the predicted ripple height (η) have been used as for the TKE-model, but k_s has been determined from the rule $k_s = \max(\eta, D_{90})$. For consistency with the Bikjer formulation, the settling velocity has been based simply on the median diameter (D_{50}) of the bed material. As noted earlier, in Bijker's model the superimposition of even small waves on a current

produces greatly enhanced bed shear stresses and, hence, transport rates. This is reflected in the quite large differences between the transport predictions of the TKE and Bijker models, particularly for small values of the current (U_c) combined with the respective waves. A more regular pattern of transport curves is produced by the Bijker model than by the TKE-model, with less overlapping occurring on account of the variations in k_s .

The results in Figures 1 to 3 provide an illustration of the variation between different modelling approaches, and of the substantial influence of the choice of bed roughness (k_s).

WAVES INCIDENT ON A BEACH

The importance of the bed roughness, and its spatial variation, for morphodynamic computations is considered, finally, with reference to waves incident on a uniform, plane sloping beach. The TELEMAC Modelling System (v5p2) has been used here to represent waves incident on a 1km length of beach. The model domain extends to a distance of 200 m offshore where the depth (at $y = 200$ m) is 10 m. The depth then decreases linearly to zero at the shoreline ($y = 0$ m).

At the outer boundary ($y = 200$ m), the waves (simulated using the module TOMAWAC) have height 1 m, peak frequency 8 s, and direction to the shoreline of either 0° (normal incidence) or 45° (oblique incidence). Wave dissipation occurs as a result of both breaking and bottom friction. There is zero wind stress. The converged model solution simulates the evolution of the wave height, frequency and direction as the waves propagate towards the beach. Figure 4a shows the cross-shore variation in wave height, for both the 0° and 45° cases, along the centre-line of the model domain ($x = 500$ m). In the case of normal incidence the wave height increases steadily towards the break point at about $y = 160$ m, beyond which it decreases rapidly towards the shoreline. In contrast, in the case of oblique incidence, the effect of the changing wave direction results in rather little variation in wave height until the waves break at about $y = 165$ m. Also shown in Figure 4a (dashed lines) is the variation in the predicted mean water level resulting from set-up and set-down. The set-up at the shoreline is quite small, amounting to 0.08 m and 0.07 m in the cases of normal and oblique incidence, respectively. The choice of lateral boundary conditions ensured that the wave conditions were very nearly uniform in the longshore direction.

In the case of oblique (45°) wave incidence, the radiation stresses give rise to a longshore current (simulated here with the module TELEMAC2D). The converged, time-mean velocity profile, which is also very nearly uniform in the longshore direction, is shown in Figure 4b. The maximum value of longshore velocity (2.4 ms^{-1}) occurs within the breaker zone (at $y = 175$ m) in water of depth 1.25 m. Lateral diffusion results in the longshore current being present well beyond the break point.

The physical picture represented by the waves and currents in Figures 4a and 4b, respectively, has been used to predict sediment transport rates. For this purpose, the model of Bijker (1971) has been implemented. This is one of the options available in the module SISYPHE. For simplicity, a single sediment size has been assumed having $D_{50} = D_{90} = 0.3$ mm. Since the Bijker model assumes that the bed roughness k_s is equal to $\max(\eta, D_{90})$, but

does not include a procedure for the calculation of the ripple height (η), the procedure outlined earlier for the calculation of ripple dimensions has been implemented *locally* within SISYPHE to estimate the variation of η , and hence k_s through the domain. It should be noted that linear wave theory has been used to calculate near-bed velocity amplitudes, based on the wave heights in Figure 4a, throughout the domain. Although this will probably have led to some inaccuracy in η , and hence k_s , within the surf zone, the trends in the results for k_s shown in Figure 5 are as expected.

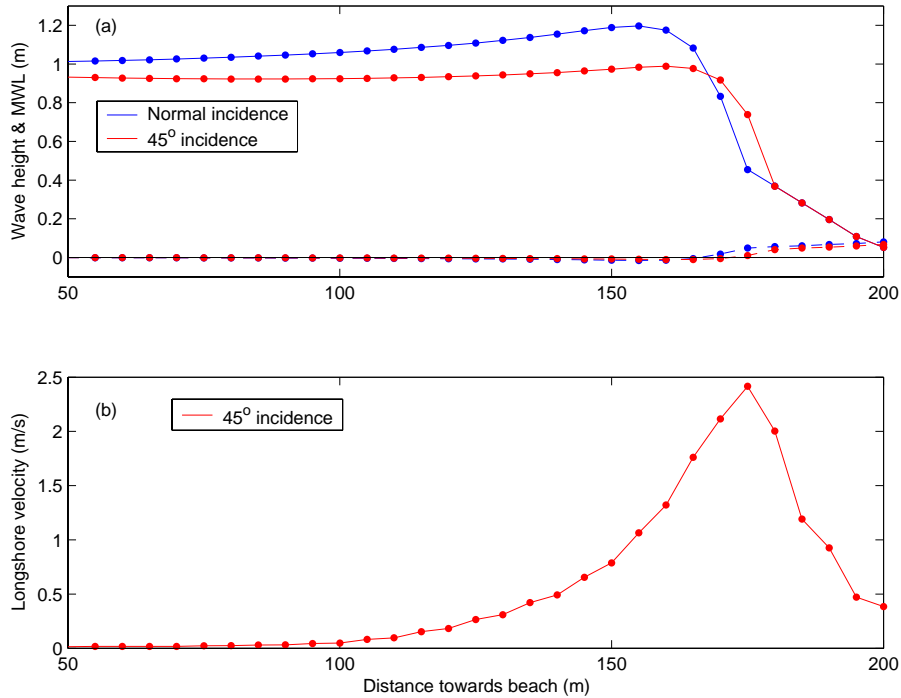


Fig. 4. Cross-shore profiles of (a) wave height and mean water level (MWL), and (b) longshore mean velocity.

For normal wave incidence, the ripples at the edge of the model domain ($y = 200$ m) are predicted to have heights of about 0.06 m. As the water depth decreases and the wave height increases, the ripple height decreases successively to about 0.02 m at $y = 120$ m, and 0.01 m at $y = 160$ m (i.e. close to the break point). Thereafter, as the wave height decreases, the ripple height increases rapidly towards the shoreline, where it again reaches values of about 0.06 m. [The decrease in k_s in the immediate vicinity of the shoreline may be anomalous.] The predicted variations in k_s as the waves shoal and then break are evidently very substantial.

For oblique wave incidence, the variations in k_s are initially less pronounced than in the case of normal incidence, the ripple height decreasing to only about 0.03 m at $y = 120$ m due to the smaller wave height in the outer region. However, the generation of the longshore current has a significant effect on the bed forms in this case, with sheet flow conditions ($k_s = D_{90}$) predicted to occur beneath the longshore 'jet' ($y = 165$ -180 m). In the inner surf zone the roughness is again predicted to increase quite sharply.

The impact on the total longshore sand transport rate of these local roughness variations is shown in Figure 6 for the oblique case. Here the profile of predicted longshore transport rate based upon the roughness variations in Figure 5 is compared with equivalent profiles from module SISYPHE based upon ‘representative’ values of the bed roughness ($k_s = 0.01, 0.02$ and 0.04 m, see Figure 5) that are assumed to be *constant* throughout the model domain. [As noted above, Bijker’s sand transport formulation has been used here; somewhat different results would have been obtained had, say, the TKE-model been used for this purpose.] The transport rate is halved approximately if local roughness variations are taken into account, compared with the results obtained assuming a uniform roughness. One of the effects of the inclusion of local variations in k_s is to produce a slight reduction in the transport rate from $y = 160$ to 165 m as a result of the predicted onset of sheet flow conditions beneath the longshore jet. The three cross-shore profiles of transport rate based on uniform roughness show relatively little variation with k_s . Maximum transport is predicted at the centre of the jet ($y = 175$ m), as expected, whatever is assumed for the roughness; here Bijker’s model actually predicts a small decrease in the transport as k_s increases from 0.01 to 0.04 m.

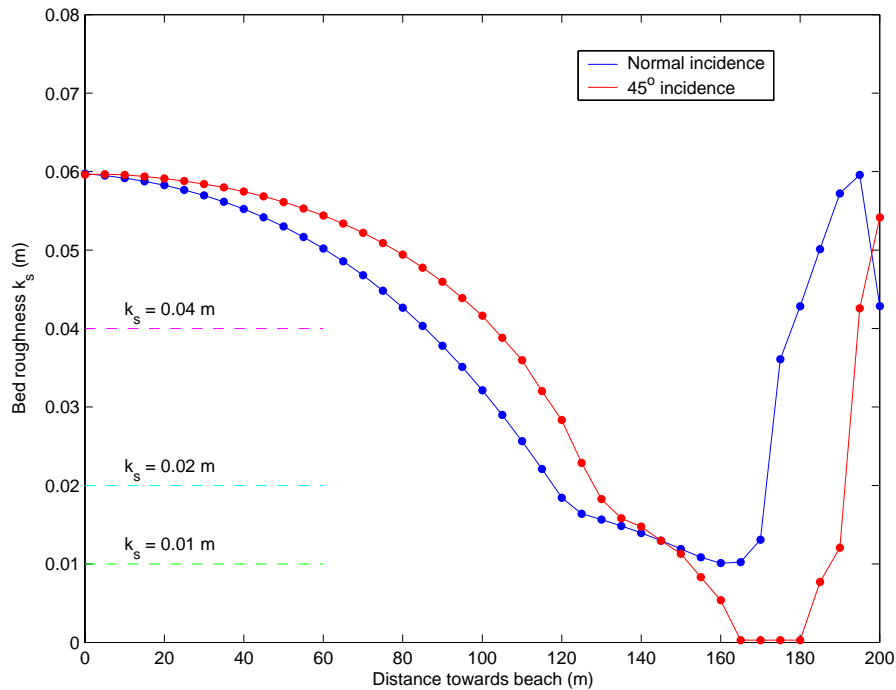


Fig. 5. Cross-shore profiles of predicted bed roughness (k_s) for the cases of normal and oblique wave incidence, together with the 3 representative values of k_s used in Figure 6.

Although the variations in longshore transport rate highlighted in Figure 6 are substantial, they have no particular significance for morphological evolution in the present simple case. However, the results do suggest that, in general cases involving topographic changes (e.g. bars, pits or banks) within the model domain, neglect of local roughness variations may lead to substantial errors in transport rates that may, in turn, affect the morphological outcome when long-duration simulations are made. Such simulations are presently being undertaken using a modified version of the SISYPHE module, in order to assess the impact on morphological

outcomes of the temporal evolution of the local bed roughness (i.e. k_s variations in space and time). Use of variations in k_s such as those proposed by Van Rijn (1993) (see Table 2) would appear to be along the right lines, and to be far preferable to assuming a uniform bed roughness throughout the model domain. However, the differences in the predictions of transport rates between Figures 1 and 2 (prescribed and predicted k_s , respectively) serves to highlight the sensitivity of transport results to the detailed variations in k_s that may occur on site. Moreover, morphological models require robust, easily implemented, and well validated prediction schemes for ripple dimensions, rather than *ad hoc* assumptions based upon the modeller's intuitions. At the present stage of research, there remains a need for improved prediction schemes of this kind.

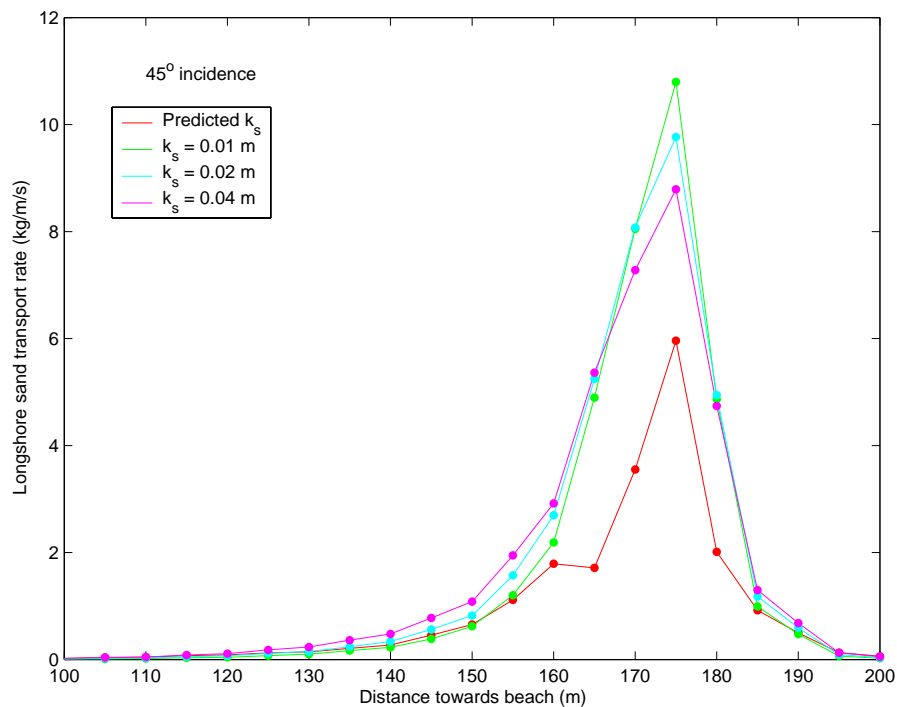


Fig. 6. Cross-shore profiles of total longshore sand transport rate predicted by Bijker's (1971) sand transport model, using the predicted and representative (constant) values of k_s indicated.

CONCLUSIONS

In the coastal zone, substantial variations in the bed roughness (k_s) are likely to have a major effect on local sand transport rates. This has been demonstrated here by a comparison involving a turbulence-closure TKE-model that has been run over a wide range of wave and current conditions. Initially, the bed roughness has been *prescribed* in a qualitatively realistic, but somewhat *ad hoc* manner, leading to a set of predictions for the total sand transport rate. Then, for the same set of conditions, the roughness has been *predicted*, using a ripple prediction scheme for waves and currents. Using these predicted roughnesses, a rather different set of transport curves is produced by the TKE-model. A further comparison over the same range of wave and current conditions has been carried out using Bijker's (1971) sand transport model. This produces significantly different predictions compared with the TKE model, giving insight into the consequences of adopting different sand transport models.

A comparison involving waves incident on a plane sloping beach has been presented to highlight the expected variation in the bed roughness as waves approach the shoreline. Here the TELEMAC Modelling System has been used to generate the wave field, for both normal and oblique wave incidence. In the latter case, a wave-induced longshore current is generated by the radiation stresses. The predicted cross-shore variations in bed roughness are substantial, with ripples of height 0.06 m being predicted outside the breaker line, and plane bed (sheet flow) conditions being predicted beneath the longshore 'jet'. The longshore sand transport rate given by Bijker's model, based on the predicted, locally varying bed roughness is about one half of that obtained by use of a representative, constant value of k_s throughout the model domain, highlighting the sensitivity of nearshore transport predictions to the choice of k_s .

From the point of view of morphological modellers, it is tempting to argue that detailed changes in sand transport rates resulting from *local* roughness variations may have little impact upon the final morphological outcome. However, this proposition needs to be tested for a range of coastal scenarios before it can be accepted. The morphological outcome will depend additionally, of course, on the choice of sand transport model. Fortunately, as demonstrated by Davies et al. (2002), most research and practical sand transport formulations exhibit a similar general behaviour, over a wide range of wave and current conditions. However, if the bed roughness on site is not known, morphological modellers should be conscious of the fact that much uncertainty still exists in relation to sand transport rate predictions, and also that more robust, validated methods are still required for the prediction of ripple dimensions and, hence, the bed roughness

ACKNOWLEDGEMENTS

This work was carried out (by AGD) as part of the EU 5th Framework SANDPIT Project No. EVK3-CT-2001-00056.

REFERENCES

- Andersen, K.H., and Fredsøe, J. 1999. How to calculate the geometry of vortex ripples. *Proceedings Coastal Sediments '99*, ASCE, 78-93.
- Bijker, E.W. 1971. Longshore transport computations. *Journal of Waterways, Harbours and Coastal Engineering Division, ASCE*, 97(WW4): 687-701.
- Bijker, E.W. 1992. Mechanics of sediment transport by the combination of waves and current. *Proceedings 23rd International Conference on Coastal Engineering*, ASCE, 147-173.
- Block, M.E., Davies, A.G., and Villaret, C. 1994. Suspension of sand in oscillatory flow above ripples: discrete vortex model and laboratory experiments. In: Belorgey, M., Rajaona, R.D., Sleath, J.F.A. (Editors), *Sediment Transport Mechanisms in Coastal Environments and Rivers*, World Scientific, Singapore, 37-52.
- Blondeaux, P., and Vittori, G. 1991. Vorticity dynamics in an oscillatory flow over a rippled bed. *Journal of Fluid Mechanics*, 226: 257-289.
- Davies, A.G., and Li, Z. 1997. Modelling sediment transport beneath regular symmetrical and asymmetrical waves above a plane bed. *Continental Shelf Research*, 17(5): 555-582.
- Davies, A.G., and Thorne, P.D. 2002. 1DV-model of sand transport by waves and currents in the rippled bed regime. *Proceedings 28th International Conference on Coastal Engineering*,

- Cardiff, ASCE. In Press.
- Davies, A.G., and Villaret, C. 1997. Oscillatory flow over rippled beds: Boundary layer structure and wave-induced Eulerian drift. In: Hunt, J.N. (Editor), *Gravity Waves in Water of Finite Depth, Advances in Fluid Mechanics*, Computational Mechanics Publications, Southampton, UK, 215-254.
- Davies, A.G., and Villaret, C. 1999. Eulerian drift induced by progressive waves above rippled and very rough beds. *Journal of Geophysical Research*, 104: 1465-1488.
- Davies, A.G., and Villaret, C. 2000. Sand transport by waves and currents: predictions of research and engineering models. *Proceedings 27th International Conference on Coastal Engineering*, Sydney, ASCE, 2481-2494.
- Davies, A.G., and Villaret, C. 2002. Prediction of sand transport rates by waves and currents in the coastal zone. *Continental Shelf Research*, 27: 2725-2737.
- Davies, A.G., Ribberink, J.S., Temperville, A., and Zyserman, J.A. 1997. Comparisons between sediment transport models and observations made in wave and current flows above plane beds. *Coastal Engineering*, 31: 163-198.
- Davies, A.G., Van Rijn, L.C., Damgaard, J.S., van de Graaff, J., and Ribberink, J.S. 2002. Intercomparison of research and practical sand transport models. *Coastal Engineering*, 46: 1-23.
- Fredsøe, J., Andersen, K.H., and Sumer, B.M. 1999. Wave plus current over a ripple-covered bed. *Coastal Engineering*, 38: 177-221.
- Fredsøe, J., and Deigaard, R. 1992. *Mechanics of Coastal Sediment Transport*, World Scientific, Singapore, 369pp.
- Hansen, E.A., Fredsøe, J., and Deigaard, R. 1994. Distribution of suspended sediment over wave-generated ripples. *Journal of Waterway, Port, Coastal and Ocean Engineering*, 120: 37-55.
- Longuet-Higgins, M.S. 1981. Oscillating flow over steep sand ripples. *Journal of Fluid Mechanics*, 107: 1-35.
- Malarkey J., and Davies, A.G. 2002. Discrete vortex modelling of oscillatory flow over ripples. *Applied Ocean Research*, 24(3): 127-145.
- Malarkey J., and Davies, A.G. 2003. A non-iterative procedure for the Wiberg and Harris (1994) oscillatory sand ripple predictor. *Journal of Coastal Research*. In Press.
- Nielsen, P. 1992. *Coastal bottom boundary layers and sediment transport*, World Scientific Publishing Co., Singapore, 324 pp.
- Sleath, J.F.A. 1991. Velocities and shear stresses in wave-current flows. *Journal of Geophysical Research*, 96(C8): 15237-15244.
- Tanaka, H., and Dang, V.T. 1996. Geometry of sand ripples due to combined wave-current flows. *Journal of Waterway, Port, Coastal and Ocean Engineering*, 122(6): 298-300.
- Van Rijn, L.C. 1993. *Principles of sediment transport in rivers, estuaries and coastal seas*. Aqua Publications, Amsterdam.
- Van Rijn, L.C., Davies, A.G., van de Graaff, J., and Ribberink, J.S. (Editors) 2001. *SEDMOC: Sediment Transport Modelling in Marine Coastal Environments*. Aqua Publications, Amsterdam, 415pp.
- Wiberg, P.L., and Harris, C.K. 1994. Ripple geometry in wave-dominated environments. *Journal of Geophysical Research*, 99(C1): 775-789.